Available online at www.sciencedirect.com
ScienceDirect
Journal of Power Sources 162 (2006) 1421–1430
JOURNAL OF POWER SOURCES
www.elsevier.com/locate/jpowsour

Miniaturized *g*- and spin-activated $Pb/HBF_4/PbO_2$ reserve batteries as power sources for electronic fuzes

Sang-Hee Yoon *, Joong-Tak Son, Jong-Soo Oh

Fuze Laboratory, Agency for Defense Development, Yuseong P.O. Box 35-5, Daejeon 305-600, Republic of Korea

Received 12 June 2006; received in revised form 25 July 2006; accepted 25 July 2006
Available online 1 September 2006

Abstract

This paper discusses miniaturized $Pb/HBF_4/PbO_2$ reserve batteries (MRB) for military applications as in-flight power sources for small-caliber electronic fuzes, where the setback acceleration and high-spin force in firing environments are used to activate the MRB. The MRB is composed of a series configured 23 bipolar electrodes, an isolated glass ampoule filled with an electrolyte and an internal cutter for breaking the glass ampoule. The MRB is designed to furnish high-voltage electrical energy with a fast activation time in gunfire environments and must have a 20-year shelf life. The electrolyte volume is determined from the simulation results of a CFD program (FLUENT) for reduction in design time and cost. Two kinds of MRBs have been designed and fabricated: MRB-S with one narrow electrolyte-filling microchannel and MRB-D with two. In the experimental study, spin tests under $10{,}000 \times g$'s and ~20,000 rpm conditions and a fire test under $43{,}000 \times g$'s and 57,000 rpm conditions have been made. The fabricated MRB with a diameter of 16 mm and a height of 13 mm has achieved a maximum voltage of 34.6 ± 0.4 V, an activation time of 8.6 ± 0.6 ms and a maximum capacity of 37.4 ± 0.4 W s at an optimized electrolyte volume of 180 mm^3. The test results have verified that the activation time of the MRB at a low temperature of −32 °C can be improved by decreasing the flow resistance of the electrolyte in spite of the decreased ion mobility.

Keywords: Activation; Bipolar electrode; Fuze; MEMS; Reserve battery; Series stack

1. Introduction

An electronic fuze, which depends on events of an electronic nature for its safety, arming and firing functions [1], requires electrical energy for operating as a component of ammunition. Designing a power source is therefore indispensable in the development of the electronic fuze. For small-caliber electronic fuze applications, an in-flight power source should satisfy the following requirements: miniaturized size, sufficient electrical energy having certain current and voltage characteristics for a given period of time, shock survivability in high-*g* environments and a 20-year shelf life. With advances in micromachining technology, MEMS has been a very powerful means for fabricating the miniaturized power sources for electronic fuzes.

Power sources used in the electronic fuzes can be classified into wind-driven generators [2], piezoelectric generators [3], inertia generators [4] and microbatteries [5–7]. Previously, wind-driven generators showed too large a volume to be fitted into the small-caliber electronic fuzes. The piezoelectric generators had much loss in storing energy in the capacitor of the electronic fuzes. The inertia generators yielded a limited electrical energy harvest in spite of the fast activation time. Recently, miniaturized and lightweight microbatteries have been developed. The microbatteries, however, show low electrical characteristics and are expected to yield performance deterioration at low temperature. The electronic fuze application requires a reserve battery for its power source because the electronic fuze's power source is integrally packaged into the fuze and is stored without possible replacement during its shelf life. In order to supply electrical energy to the electronic fuze of small-caliber ammunitions, a reserve-type power source should satisfy the above-mentioned requirements and the fast activation time of ~50 ms at the temperature range of −32 to +60 °C, which is compliant with the environmental conditions of MIL-STD-331B [8].

In this paper, new class of MEMS-based *g*- and spin-activated $Pb/HBF_4/PbO_2$ reserve batteries with fast activation times at low

* Corresponding author. Tel.: +82 42 821 4127; fax: +82 42 821 2390.
E-mail address: shyoon@add.re.kr (S.-H. Yoon).

0378-7753/$ – see front matter © 2006 Elsevier B.V. All rights reserved.
doi:10.1016/j.jpowsour.2006.07.051

temperatures are designed and fabricated to provide electrical energy for small-caliber electronic fuzes. Instead of a lithium-based battery ($Li/SOCl_2$ battery), a $Pb/HBF_4/PbO_2$ electrochemical system is used because the former shows a slow activation time of ~250 ms, while the latter has a fast activation time of ~100 ms at low temperature [9]. Miniaturized reserve batteries (MRB) with a diameter of 16 mm and a height of 13 mm have four features: first, the MRB is intended to take advantage of *the setback acceleration and spin force in gunfire environments* to activate the MRB and keep an electrolyte within the reaction sites. Second, *the bipolar electrode plates* of the MRB are stacked in a *series configuration* to furnish the high-voltage output of ~35 V in a very small space. Third, *the electrolyte volume* of the MRB is optimized on the basis of *the simulation results of a CFD program*. Fourth, *the spacers* of the MRB are designed to *reduce the flow resistance of the electrolyte* in the microchannels for a *fast activation time at low temperature*.

2. Theory of operation

A reserve battery generally consists of an electrode stack, a glass ampoule, an electrolyte within the glass ampoule, and a housing assembly. The *g*- and spin-activated miniaturized reserve battery (MRB) breaks the glass ampoule using the setback acceleration of gunfire and then distributes the electrolyte onto the reaction sites using the in-flight spin force, thereby activating the MRB and providing electrical energy to the electronic fuzes.

2.1. Structure of MRB

Fig. 1 illustrates a schematic diagram of a miniaturized *g*- and spin-activated $Pb/HBF_4/PbO_2$ reserve battery that consists of an electrode stack, a glass ampoule housing the electrolyte of HBF_4, an internal cutter and a housing assembly. The electrode stack of annular shape composed of Pb negative electrodes, PbO_2 positive electrodes, impervious spacers, a cathodic collector and an anodic collector is isolated from the electrolyte before gunfire and provides electrochemical reaction sites after gunfire. The dry-packaged electrode stack makes it possible to preserve the performances of the MRB for a 20-year shelf life. The electrode stack is in annular shape to make the electrolyte flow into the reaction sites by the in-flight centrifugal force. To minimize the volume of the electrode stack and reduce the intercell ohmic resistance, the electrode stack is made of bipolar plates where the anode of unit cell 1 is on one side of a conductive plate and the cathode of unit cell 2 is on the other side of the same plate. To meet the voltage requirement of more than 30 V for small-caliber electronic fuzes, the bipolar electrode plates are stacked in a series configuration. In the present MRB, the spacers in an annular shape seal the outer peripheries of the electrodes. The spacers are used as supports for the cavity between the bipolar electrode plates, and are barriers for keeping the electrolyte from leaking out, and act as insulators for preventing intercell short circuits which are caused by deformation of the bipolar electrode plates in gunfire environments.

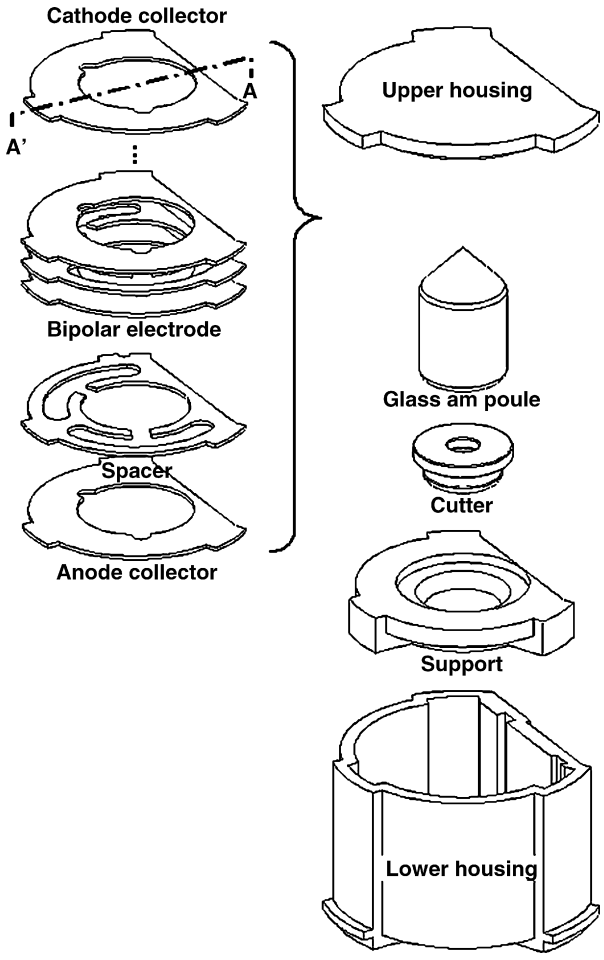

Fig. 1. Schematic representation of miniaturized *g*- and spin-activated $Pb/HBF_4/PbO_2$ reserve battery showing that 23 bipolar electrodes (2 dummy cells included) are stacked in a series configuration to furnish high-voltage output.

The glass ampoule is used to keep the electrolyte stack dry before gunfire and therefore makes the long-term storage of the MRB possible by isolating the electrode stack from the electrolyte. The internal cutter is not only a safety device to prevent the MRB from being activated by rough handlings but also a striker to puncture the glass ampoule upon gunfire.

2.2. Working principle of MRB

The MRB is an electrochemical system composed of Pb, HBF_4 and PbO_2. To make long-term storage possible, the HBF_4 electrolyte is stored in the glass ampoule and isolated from the electrode stack because the Pb and PbO_2 electrodes in general are severely corroded by the HBF_4 electrolyte. On gunfire, the electrolyte in the glass ampoule is released and distributed into the electrode stack, thereby making the $Pb/HBF_4/PbO_2$ electrochemical system complete.

The operational process of the MRB is shown in Fig. 2. Before gunfire (Fig. 2a), the glass ampoule inserted in the center hole of the electrode stack houses the electrolyte, thereby keeping the MRB deactivated. The setback force and centrifugal force that a projectile fired by a rifled gun experiences are the driving forces

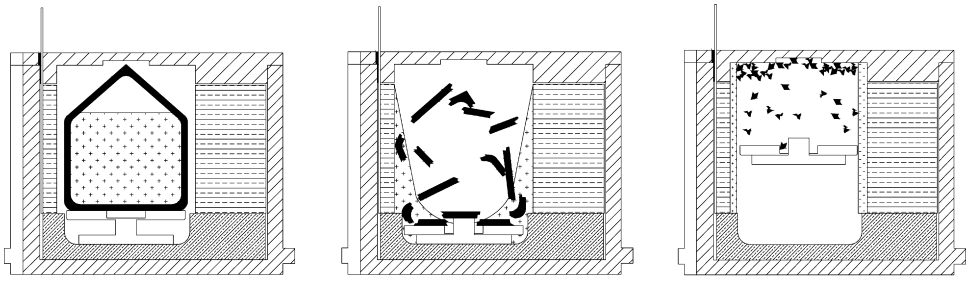

Fig. 2. Working principle of miniaturized $Pb/HBF_4/PbO_2$ reserve battery in A–A′ cross section (refer to Fig. 1): (a) before gunfire, electrolyte within glass ampoule is isolated from electrode stack; (b) upon gunfire, glass ampoule housing electrolyte smashes against internal cutter by setback acceleration and electrolyte is released by centrifugal force; (c) during flight, released electrolyte is distributed into cells by centrifugal force and MRB starts working.

for activating the MRB, which satisfy the two independent safety features of MIL-STD-1316E [10]. Upon gunfire that accompanies the setback acceleration of 43,000 × g's (Fig. 2b), the upper plate of the I-type internal cutter is sheared and moved down by the setback force. A protruding awl is smashed against the glass ampoule and the electrolyte within the glass ampoule is released. For reference, the glass ampoule is not broken by careless handling because the glass ampoule is designed to endure the shock by a drop on a hard surface. During flight that accompanies the spin of 57,000 rpm (Fig. 2c), the electrolyte is distributed into the electrode stack by the centrifugal force and drag force. The centrifugal force-driven flow of the electrolyte pushes out the air bubbles generated during electrochemical reaction at the microchannels and increases the wetting areas, or reaction sites. This is because the flow at a rotational velocity of 57,000 rpm has enough centrifugal force to overcome the surface tension of the air bubbles, although the surface tension is one of the most dominant forces in the micro domain [11–13]. The released electrolyte makes the MRB generate electrical energy. Fig. 3 shows the equivalent circuit of the MRB where UC_n is the nth unit cell in series configuration, S_n is the nth interconnection between UC_n and UC_{n+1}, and S_s is an imaginary interconnection that causes the intercell short circuits. The released electrolyte of optimized volume makes all interconnections S_n except the imaginary interconnection S_s be ON between unit cells, providing the series configured electrode stack with the continuity.

2.3. Chemistry of MRB

The electrochemical reaction at lead electrode of the MRB, anodic reaction (oxidation), is written as [14]

$$Pb + 2BF_4^- \Rightarrow Pb(BF_4)_2 + 2e^- \quad (1)$$

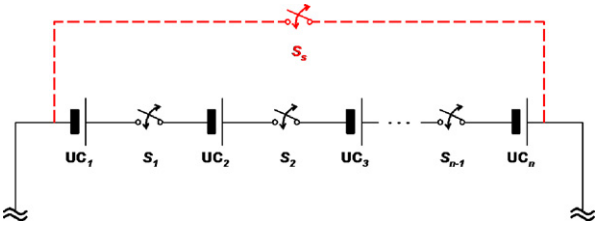

Fig. 3. Equivalent circuit of miniaturized $Pb/HBF_4/PbO_2$ reserve battery where UC_n is nth unit cell in series stacked MRB and S_n is nth interconnection between UC_n and UC_{n+1}.

The cathodic reaction (reduction) at lead dioxide is expressed as

$$PbO_2 + 4H^+ + 2BF_4^- + 2e^- \Rightarrow Pb(BF_4)_2 + 2H_2O \quad (2)$$

The total reaction (discharge) of the MRB is therefore represented as

$$Pb + PbO_2 + 4HBF_4 \Rightarrow 2Pb(BF_4)_2 + 2H_2O \quad (3)$$

The theoretical equilibrium voltage of the MRB unit cell can be calculated from the thermodynamic values of free enthalpy based on Gibbs free energy [15]. The calculation yields the standard value observed under the standard conditions of 25 °C and 1 atm.

$$E^\circ = \frac{-\Delta G^\circ}{mF} \quad (4)$$

where E°, ΔG°, m and F are the standard potential, the decrease in the free enthalpy of the unit cell under standard conditions, the number of electrons involved in stoichiometric reaction and Faraday constant defined as 96,500 Coulombs or 26.8 Ah, respectively. The decrease in the free enthalpy of reaction in (4) may be written as

$$\Delta G^\circ = 2G^\circ_{Pb(BF_4)_2} + 2G^\circ_{H_2O} - G^\circ_{Pb} - G^\circ_{PbO_2} - 4G^\circ_{HBF_4} \quad (5)$$

where ΔG_i° is the free enthalpy decrease related to material i. On the basis of (4) and (5) and the standard potentials in Table 1, the theoretical equilibrium voltage of the MRB unit cell is calculated as 1.86 V.

Theoretical capacity, Q_{cap}, of the MRB unit cell can be also derived from the electrochemical reaction shown in (3). The theoretical capacity is on the hypothesis that the theoretical

Table 1
Free enthalpies and atomic weights of chemical materials used in MRB

Material	G° (kJ mol^{-1})	Atomic weight (g mol^{-1})
Reagent		
Pb	0	207.2
PbO_2	−219.2	239.2
HBF_4	−1487.0	87.8
Product		
$Pb(BF_4)_2$	−2666.8	380.8
H_2O	−237.4	18.0

equilibrium voltage is related to the activity of 1 mol l^{-1}. The theoretical capacity is determined from the amounts of active materials in the unit cell.

$$Q_{cap} = \frac{nF}{\sum \text{molar weight of reaction participants}} \quad (6)$$

Using (6) and atomic weights in Table 1, the theoretical capacity is calculated as 67.2 Ah kg^{-1}. The hypothetical specific energy, E_s, is therefore amounted as $E_s = E^\circ Q_{cap} = 124.9$ Wh kg^{-1}. The theoretical equilibrium voltage and hypothetical specific energy of unit cell in the MRB are respectively 1.86 V and 124.9 Wh kg^{-1} that are roughly equivalent to the practical values of 1.6 V and 135 Wh kg^{-1} of a commercial silver oxide primary battery, $Ag_2O/H_2O/Zn$ battery system [15].

3. Design and fabrication

Linear high-g acceleration (setback acceleration) and high-spin force, such as those encountered in gunfire environments, may put restrictions on designing of power sources for small-caliber electronic fuzes. The present miniaturized g- and spin-activated $Pb/HBF_4/PbO_2$ reserve batteries are, however, designed to make use of the setback acceleration and high-spin force for activating the MRB and keeping the electrolyte within the reaction sites, respectively.

Two kinds of MRBs including MRB-S and MRB-D are designed as shown in Fig. 4. The MRB-S is a fundamental prototype with one 20°-inflow window and the reaction area of 46.9 mm^2, while the microchannels of the MRB-D are defined by two 20°-inflow windows and the reaction area of 46.1 mm^2. The MRB-D is intended to examine the effect of total window size on the activation time by making the electrolyte uniformly distributed. The structure of microchannels and the optimum volume of electrolyte are important design factors to determine the performance of the MRB. The heart of this research is therefore placed on defining the microchannels and determining the optimum volume of electrolyte to reduce the activation time in low-temperature gunfire environments. For the electrode stack, bipolar plates are connected in series to furnish the high-voltage output and minimize the intercell ohmic resistance. Based on the voltage requirements of more than 30 V, 23 unit cells (2 dummy cells included) are stacked in series configuration in consideration of ohmic drops in the electrode and electrolyte. The bipolar plates in an annular shape make the electrolyte flow easily into the reaction sites by centrifugal force. For spacer shown in Fig. 4, an impervious paper with plastic coating is punched to seal the outer peripheries of the electrodes because the electrolyte leaks from the electrode stack by in-flight centrifugal force without sealing. To reduce and uniform the activation time of the MRB at the low temperature of −32 °C, the microchannels supported by the spacers should be designed to maximize the flow-rate of the electrolyte. In general, the activation time at low temperature gets slowed due to the increase in the electrolyte viscosity and the decrease in the ion mobility. The design of the spacer is focused on not increasing the ion mobility, which is hard to control, but minimizing the effect of the viscosity increase. To make the activation time faster, the shape of spacer is elaborately designed to reduce the time for distributing the electrolyte in the MRB. The inner peripheries of the spacers of MRB-S and MRB-D are designed to have one 20° narrow inflow window and two 20° narrow inflow windows, respectively. The thickness of the spacer is 230 μm after hot pressing and the height of the microchannel is also 230 μm. The spacer of the MRB-S has almost a two-fold flow resistance, compared with that of the MRB-D [16].

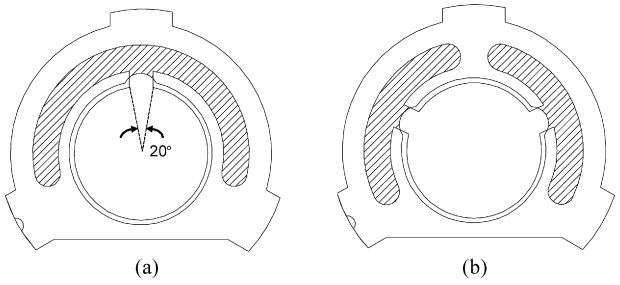

Fig. 4. Specification of spacer for defining electrolyte-distributing microchannels, where the reaction sites are indicated in hatching: (a) MRB-S prototype and (b) MRB-D prototype.

Fluoboric acid, HBF_4, is selected as the electrolyte to improve the low-temperature performance of the MRB. The fluoboric acid shows low-temperature performance better than other electrolytes such as sulfuric acid because the fluoboric acid electrolyte produces soluble discharge products when the MRB discharges [17]. This allows a higher current to be drawn at low temperatures. The concentration of fluoboric acid is determined to be 50%, which is that in commercial one. The electrolyte should be separated from the electrode stack through a glass ampoule because the corrosion of the electrodes in the fluoboric acid is too severe to be used in a primary battery, where anode, cathode and electrolyte are stored together. The glass ampoule housing the electrolyte is designed on the basis of the fracture stress of Pyrex glass. An I-type internal cutter is designed as a safety device for preventing the ampoule from being broken by the acceleration of ∼5000 × g's. Over 5000 × g's, the upper plate of the internal cutter is sheared and then the protruding awl is smashed against the glass ampoule. The internal cutter has 7.7 mm in outer diameter, 4.05 mm in total height and 0.4 mm in protruding awl's height.

In the series configured MRB, the overflowing electrolyte produces intercell short circuits in the manifold of microchannels into which the electrolyte is filled. A deficiency in the electrolyte volume, however, makes at least one unit cell empty and therefore fails to provide the continuity to the electrode stack, or supplies insufficient electrical energy although all unit cells are connected [18]. In the equivalent circuit of the MRB shown in Fig. 3, the flooding electrolyte condition provokes S_s to be ON between some unit cells, causing intercell short circuits, and the insufficient electrolyte condition leaves at least one of S_s OFF. The electrolyte volume should be therefore matched to the total volume of microchannels of the MRB. The electrolyte volume is determined from the simulation results of FLUENT. In the simulation of MRB, 3D, transient, two-phase and laminar flow model based on "volume of fluid (VOF)" is used to explore

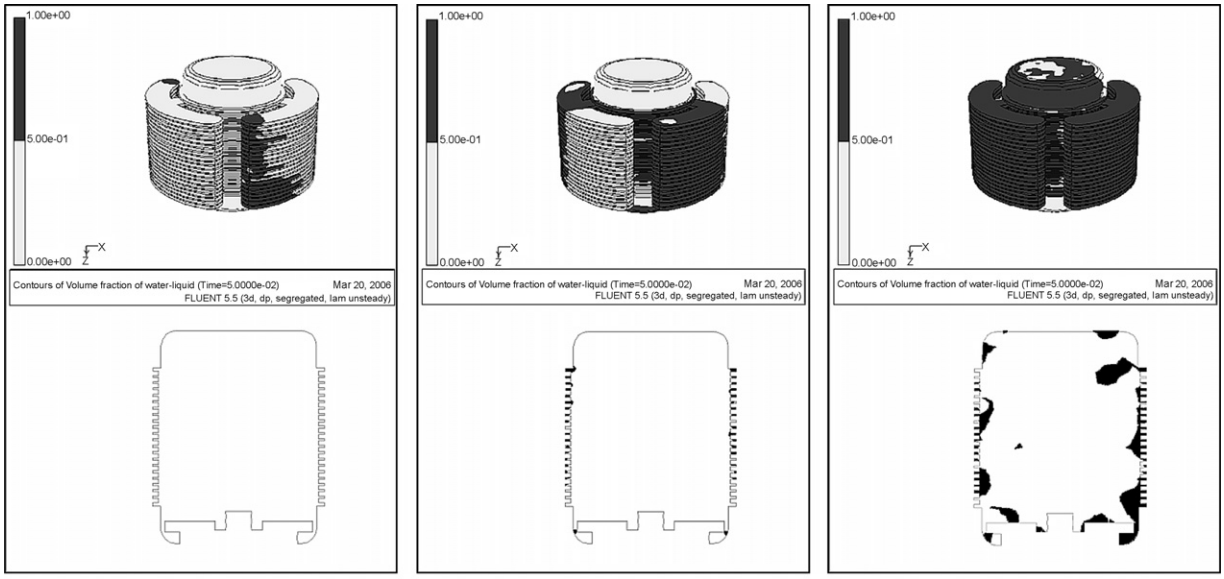

Fig. 5. Estimated electrolyte distribution of MRB-D in A–A′ cross-section (refer to Fig. 1) at time of 50 ms: (a) electrolyte volume of 45 mm^3; (b) electrolyte volume of 180 mm^3; (c) electrolyte volume of 280 mm^3.

the in-flight behavior of the electrolyte as the electrolyte is accelerated and spun by 43,000 × g's and 57,000 rpm as summarized in Table 2. FLUENT's dynamic mesh model is used in simulating the motion of the electrolyte. The VOF model assumes that two phases are immiscible and the surface separating the phases can be tracked as a function of time. FLUENT tracks the interface through computation, while the phases share a common pressure and velocity field [19]. The surface tension and wall adhesion effect are considered in the simulation. Fig. 5 illustrates the estimated electrolyte distributions in A–A′ plane of the MRB-D at the time of 50 ms. Based on the simulation results, the optimized electrolyte volume is determined to be 180–200 mm^3, maximum volume which does not bring about intercell short circuits in the MRB.

The MRB is fabricated using a standard micromachining process as shown in Fig. 6. The fabrication process of the MRB starts with a 64 ± 8 μm-thick cold rolled carbon steel plate as a substrate instead of a silicon wafer. This is because silicon is too brittle to survive in gunfire environments that accompany the high-g acceleration [20]. To fabricate the bipolar electrode, the steel plate is electroplated in $NiSO_4$:$NiCl_2$:H_3BO_3 solution to form a 6 μm-thick Ni layer as an adhesion layer for Pb and PbO_2 electroplating processes (Fig. 6a). The Ni electroplated substrate is electroplated in $2(PbCO_3)\cdot Pb(OH)_2$:HF:H_3BO_3 solution to form a 8 μm-thick Pb layer as cathodic material (Fig. 6b) and then 11 μm-thick PbO_2 layer is also electroplated in $Pb(NO_3)_2$:PbO solution as anodic one, followed by the die cutting of the electrode (Fig. 6c). To seal the unit cells and define the

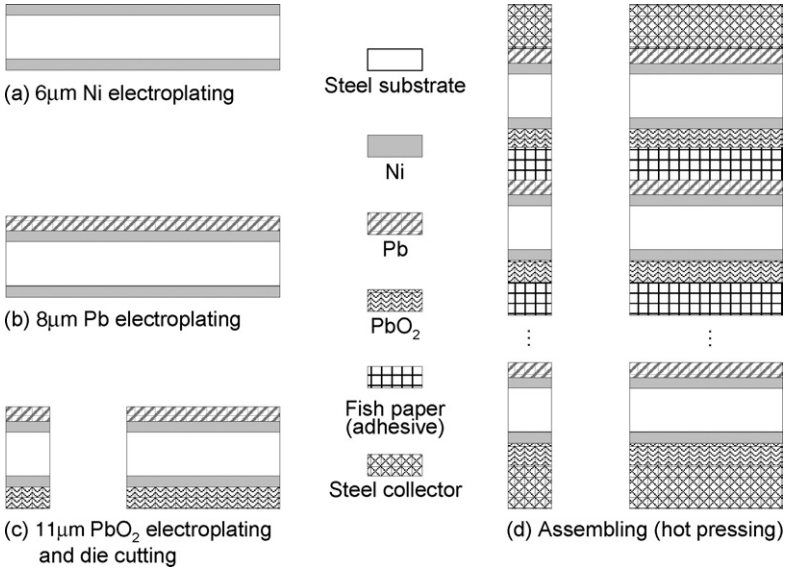

Fig. 6. Fabrication process of miniaturized Pb/HBF_4/PbO_2 reserve battery in A–A′ cross-section (refer to Fig. 1).

Table 2
Solver settings and conditions used in simulation of MRB

Model	Setting
Space	3D
Time	Unsteady
Viscous model	Laminar
Solver	Segregated, double precision
Multiphase	VOF with surface tension
Material—primary phase	Air
Material—secondary phase	Fluoboric acid, HBF_4
Viscosity	Constant (air and HBF_4)
Density	Ideal-gas (air), constant (HBF_4)
Discretization	First order, all equations
Pressure–velocity coupling	PISO
Discretization of pressure	Body force weighted

electrolyte-filling microchannels between the fabricated bipolar electrodes, Fishpaper coated with ethylene acrylic acid (EAA) copolymer is cut and placed at the interspaces of the bipolar electrodes. The cut Fishpaper and bipolar electrodes are hot pressed under a pressure of 10 bar and the temperature of 150 °C during 4 h (Fig. 6d). The ampoule is fabricated using Pyrex 7740. After pouring the electrolyte into the glass ampoule using a micropipette, the ampoule is sealed hermetically. In the assembling process, the fabricated internal cutter, the glass ampoule containing the electrolyte and the bipolar electrodes are assembled into the MRB housing.

Fig. 7 shows the scanning electron microphotographs (SEM) of the electroplated electrodes before and after improvement. Before improvement, Pb cathode has porous defects, which deteriorate the electrical characteristics of the MRB. By changing the concentration of electroplating solution and the electroplating temperature, the electrodes without porous defects are fabricated. Fig. 8 shows a picture of the fabricated MRB, which is 16 mm in diameter and 13 mm in height. The measured dimensions of the fabricated MRBs are summarized in Table 3.

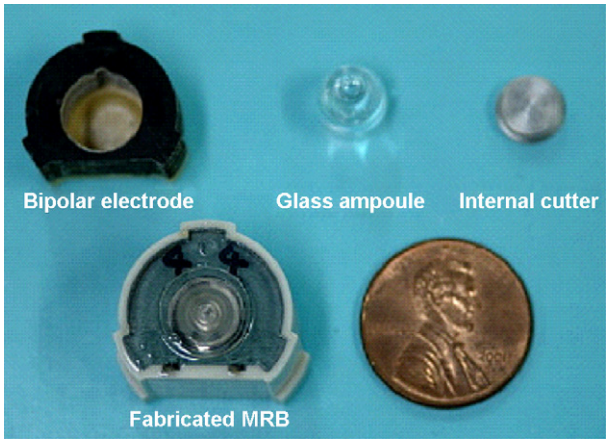

Fig. 8. Photograph of miniaturized *g*- and spin-activated $Pb/HBF_4/PbO_2$ reserve battery compared with one-cent coin, showing electrode stack, glass ampoule and internal cutter.

4. Experiment and results

In the experimental study, two classes of tests including the spin test in the laboratory and the gunfire test in field are made. The spin test is conducted under the acceleration of 10,000 × *g*'s, the rotational velocity of ~20,000 rpm and the temperatures of −32 °C (low), +18 °C (medium) and +60 °C (high) and the fire test is carried out under the acceleration of 43,000 × *g*'s, the rotational velocity of 57,000 rpm and the above-mentioned temperatures. The former is to examine the performances of the

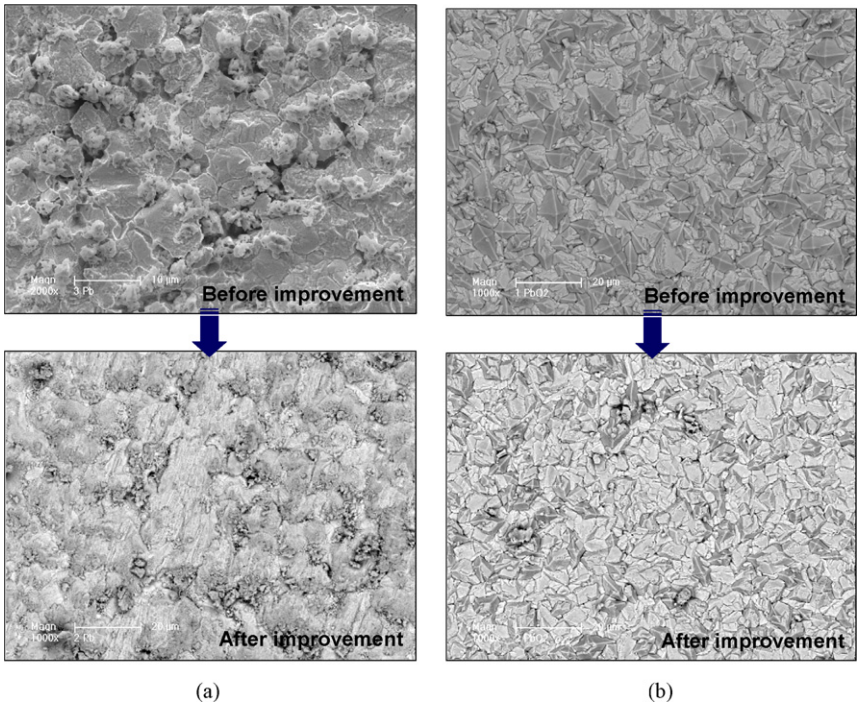

Fig. 7. Scanning electron microphotographs (SEM) of electroplated electrodes before and after improvement: (a) lead (Pb) cathode and (b) lead oxide (PbO_2) anode.

Table 3
Measures dimensions of MRB

Component	Dimension	MRB-S	MRB-D
Electrode	Number of unit cell[a]	23	23
	Reaction area per unit cell (mm^2)	46.9	46.5
Spacer	Inlet window size	20° × 1	20° × 2
	Thickness[b] (μm)	230	230
Electrolyte	Total volume (mm^3)	226.5	224.6
	Occupying volume (mm^3)	180	180
	Fill factor[c] (%)	79.5	80.1

[a] Two dummy cells included.
[b] Distance between bipolar electrodes.
[c] Ratio of electrolyte volume to total volume.

fabricated prototype MRB and to compare the experimentally determined electrolyte volume with the estimated one, while the latter is to characterize the operational characteristics and shock survivability of the fabricated MRB in gunfire environments.

4.1. Laboratory spin test

The laboratory test was carried out in the battery laboratory of the Hanwha Corporation. The experimental set-up for the spin test is illustrated in Fig. 9. The fabricated MRB assembled at a *g*- and spin-activation equipment is kept in a temperature and humidity-controlled chamber where the temperature is in the range of −32 to +60 °C and the humidity is maintained less than 20%. The axial acceleration (*g*-activation) of ∼10,000 × *g*'s required to smash the electrolyte ampoule is generated by a pneumatic pressure equipment and the centrifugal acceleration (spin-activation) required to distribute the electrolyte is applied by a dc motor having the rotational velocity of ∼20,000 rpm. The output voltage and output current of the MRB under the external load of 20 mA are measured by a LeCroy wave 7000 oscilloscope. To verify the electrolyte volume determined from the simulation results, the output voltage of the fabricated MRB is measured under the rotational velocity of 20,000 rpm and +18 °C when the electrolyte volume is changed 45 to 280 mm^3 as shown in Fig. 10. The MRB with an electrolyte volume of 180 mm^3, which agrees with the simulation results, generates

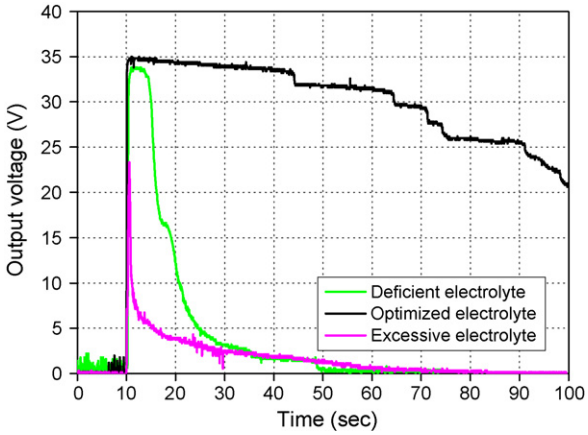

Fig. 10. Measured output voltage of MRB-D under rotational velocity of 20,000 rpm and temperature of +18 °C when electrolyte volume is changed 45 to 280 mm^3: Deficient, optimized and excessive electrolytes indicate electrolyte volume of 50, 180 and 250 mm^3, respectively.

an output voltage of 34.9 V under the external load of 20 mA, produces a useful life range of 54 s. The life range is a time when the output voltage of the MRB is more than 30 V. The life range of 54 s is sufficient time for small-caliber electronic fuzes to carry their missions in military applications. The measured practical equilibrium voltage of a unit cell of 1.67 V is less than the theoretical equilibrium voltage of 1.86 V. This is because of the ohmic drops generated in the electrodes and electrolyte.

Fig. 11 shows the measured results of the spin test as a function of electrolyte volume under the rotational velocity of 20,000 rpm and the temperature of +18 °C. The experimental results demonstrate that the electrolyte volume should be optimized on the basis of the rotational velocity to prevent the phenomena of the intercell short circuits and discontinuity on the electrode stack of the MRB. Through the spin test at room temperature, where the rotational velocity is limited to 20,000 rpm, the optimized electrolyte volume is measured to be 140–210 mm^3. This measured range shows a large deviation of ∼28.6% from that of FLUENT simulation results

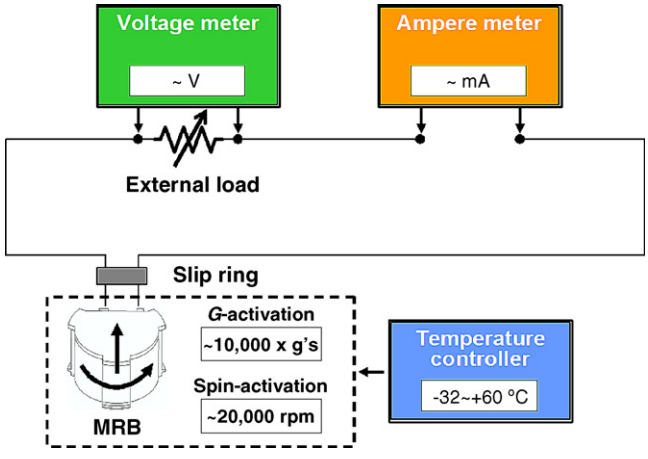

Fig. 9. Experimental set-up of laboratorial spin test.

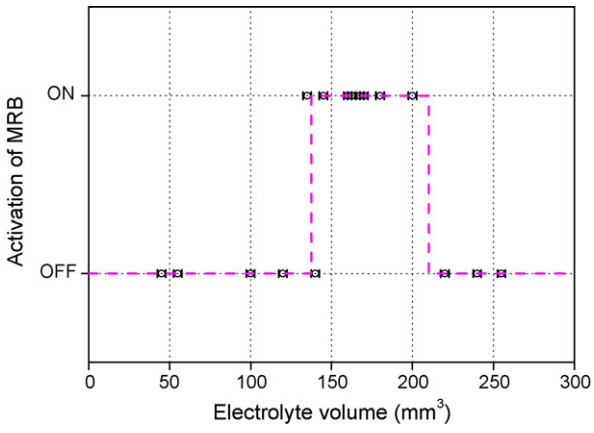

Fig. 11. Measured activation of MRB-D as function of electrolyte volume under rotational velocity of 20,000 rpm and temperature of +18 °C.

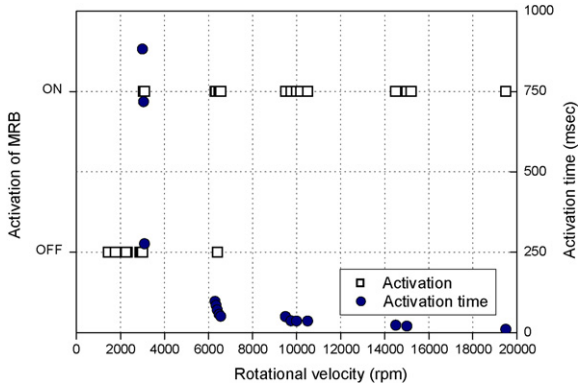

Fig. 12. Measured activation time of MRB-D as function of rotational velocity under electrolyte volume of 180 mm^3 and temperature of +18 °C, where activation time is defined as time from initiation of the MRB to point at which MRB generates the output voltage of 30 V.

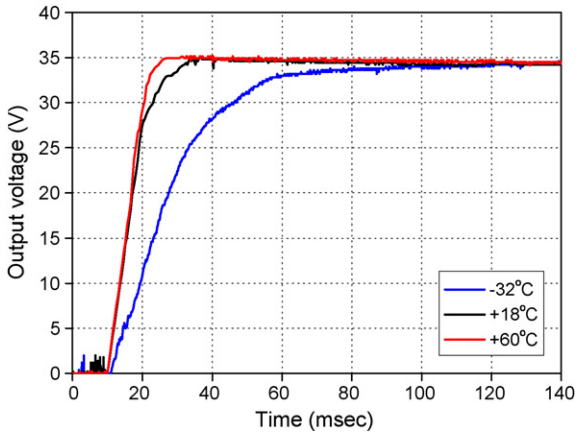

Fig. 13. Measured output voltage of MRB-D with external load of 20 mA under electrolyte volume of 180 mm^3, rotational velocity of 20,000 rpm and temperatures of −32, +18 and +60 °C.

(180–200 mm^3). This is because the rotational velocity of the spin test is limited to 20,000 rpm, while that of simulation is assumed as 57,000 rpm. The test results, however, show that designing the electrolyte volume based on the simulation results of FLUENT is reasonable although the electrolyte volume range determined by simulation is narrower than that of the laboratorial spin test. Fig. 12 illustrates the measured activation time of the fabricated MRB as a function of rotational velocity under the electrolyte volume of 180 mm^3 and the temperature of +18 °C. In this paper, the activation time of the MRB is defined as a time from initiation to the point at which the MRB generates the output voltage of 30 V. The measured results indicate that the rotational velocity of the MRB should reach a certain level to activate the MRB at a given electrolyte volume. This is because the fabricated MRB requires the centrifugal force to distribute the electrolyte into the reaction sites. The rotational velocity effect on activation time of the MRB is also shown in Fig. 12. The activation time gets shorter as the rotational velocity of the MRB gets faster because of the time reduction for distributing the electrolyte and clearing of the electrolyte short circuits in the microchannels.

To explore the temperature effect on activation time, the output voltage of the fabricated MRB is measured with varying the temperature. Fig. 13 illustrates the measured output voltage of the fabricated MRB-D with the external load of 20 mA under the electrolyte volume of 180 mm^3, the rotational velocity of 20,000 rpm and the temperatures of −32, +18 and +60 °C. The external load value is determined from the electrical requirements of small-caliber electronic fuzes under development. The activation time of the MRB gets shorter as the temperature gets higher. This is because the viscosity of the electrolyte gets decreased and the ion mobility gets increased. The electrochemical reaction velocity of the MRB therefore gets faster as the operational temperature of the MRB gets higher. The average of measured activation times of ten MRBs is summarized in Table 4. The MRB-D has the activation times of 45.0 ± 12.8, 12.3 ± 2.5 and 10.2 ± 1.9 ms, while MRB-S has 63.5 ± 38.4, 15.4 ± 4.6 and 13.1 ± 2.7 ms at the temperatures of −32, +18 and +60 °C, respectively. Owing to the lower flow resistance in the microchannels of the MRB-D, the activation times of the MRB-D are faster and more uniform than those of the MRB-S. Through the laboratorial spin test, the fabricated MRB has showed the maximum voltage of 34.6 ± 0.4 V, the activation time of 12.3 ± 2.5 ms and the maximum capacity of 37.4 ± 0.4 W s at room temperature, satisfying the general design requirements of the small-caliber electronic fuzes.

4.2. Gunfire test

To compare the performances between the MRB-S and the MRB-D in gunfire environments, the proximity-mode ammunition powered by the fabricated MRB was fired. For reference, the proximity-mode ammunition transmits an oscillating wave to detect a target and the wave's frequency is proportional to the output voltage of the MRB. The in-flight output voltage of the MRB is experimentally extracted from the measured frequency of the oscillating wave. Fig. 14 illustrates the experimental setup of the gunfire test for characterizing the fabricated MRB in the gunfire environments of 43,000 × g's and 57,000 rpm. The frequency spectrum of the oscillating wave was measured by a realtime spectrum analyzer set (RSA 3303A, Tektronix) and the measurement was triggered by the signal of an infrared sensor for detecting a flame of gunfire.

Fig. 15 shows the measured frequency spectrum of the proximity-mode ammunition powered by the fabricated MRB-

Table 4
Measured activation times of MRB with respect to temperature

Test	Temperature (°C)	Activation time (ms)	
		MRB-S	MRB-D
Spin test	−32	63.5 ± 38.4	45.0 ± 12.8
	+18	15.4 ± 4.6	12.3 ± 2.5
	+60	13.1 ± 2.7	10.2 ± 1.9
Gunfire test	−32	40.8 ± 14.9	28.7 ± 6.5
	+18	14.7 ± 2.9	8.6 ± 0.6
	+60	–	7.1 ± 0.7

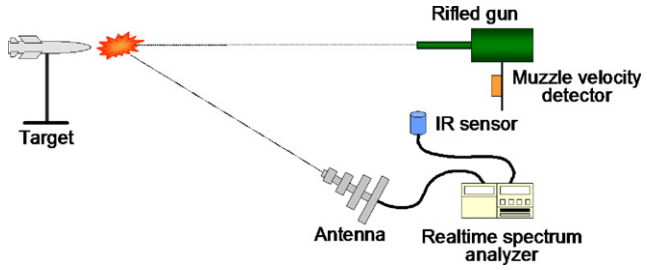

Fig. 14. Experimental set-up of gunfire test for characterizing MRB in gunfire environments.

D at the temperatures of −32, +18 and +60 °C. The frequency spectrum is normalized by the maximum frequency and the normalized frequency of 0.99 means that the output voltage of MRB-D reaches 30 V. The measured activation times of the MRB-D are 28.7 ± 6.5, 8.6 ± 0.6 and 7.1 ± 0.7 ms at −32, +18 and +60 °C, respectively. The measured activation times satisfy the requirements of the power supply for small-caliber electronic fuzes, ∼50 ms. The measured activation time of the MRB-D in gunfire environments gets slower as the operational temperature of the MRB gets lower. Compared with that of the laboratorial spin test, the activation time of the gunfire test is shorter. The reduction of activation time in gunfire environments is due to the increase in rotational velocity from 20,000 to 57,000 rpm. The optimized electrolyte volume in gunfire environments is determined to be 180–200 mm^3 or more. The electrolyte volume decided by the gunfire test quite agrees with that of FLUENT simulation results, which shows that the determination of electrolyte volume based on the simulation results of FLUENT is appropriate and can reduce the design time and cost successfully.

The comparison between the activation times of MRB-S and MRB-D is shown in Fig. 16. The measured activation times of the MRB-S are 40.8 ± 14.9 and 14.7 ± 2.9 ms at −32 and +18 °C, respectively. The measured activation times of the MRB-S are 42.2 and 70.9% longer than that of the MRB-D at low- and medium-temperatures, respectively. The measured activation times of the MRB in gunfire environments are summarized in Table 4. The test results prove that the activation time of the MRB at the low temperature of −32 °C can be improved by decreasing the flow resistance of the electrolyte in the microchannels and distributing the electrolyte faster although the ion mobility is decreased at low temperature. Through the gunfire test, the shock survivability of the MRB in the gunfire environments of 43,000 × *g*'s and 57,000 rpm was also experimentally verified.

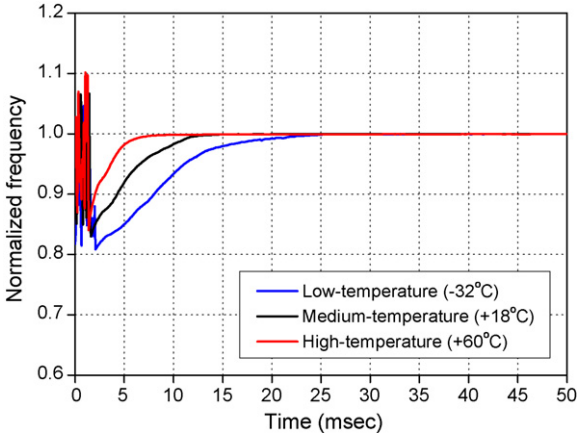

Fig. 15. Measured frequency spectrum of proximity-mode ammunition powered by MRB-D under gunfire environments of 43,000 × *g*'s and 57,000 rpm, and temperatures of −32, +18 and +60 °C, where normalized frequency of 0.99 means that output voltage of MRB-D reaches 30 V.

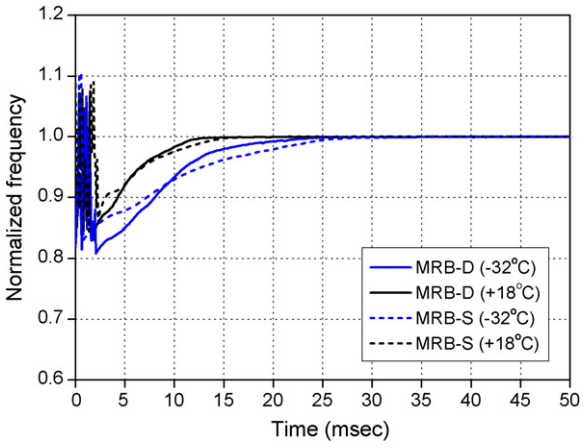

Fig. 16. Comparison between measured frequency spectrum of MRB-D and that of MRB-S under gunfire environments of 43,000 × *g*'s and 57,000 rpm, and temperatures of −32 and +18 °C.

5. Conclusions

Miniaturized Pb/HBF_4/PbO_2 reserve batteries have been demonstrated for in-flight power source of small-caliber electronic fuzes, where the setback acceleration and high-spin force in gunfire environments are used to activate the MRB. The MRB, composed of series configured 23 bipolar electrodes, a glass ampoule, an electrolyte and an internal cutter, has been designed to generate the high-voltage output of ∼35 V with the fast activation time of ∼50 ms in gunfire environments of 43,000 × *g*'s and 57,000 rpm, and to guarantee 20-year shelf life. The electrolyte volume of the MRB has been determined from the simulation results of FLUENT for reduction in design time and cost. Two kinds of MRBs have been designed and fabricated: MRB-S with one 20° electrolyte-filling microchannel and MRB-D with two. In the spin test under the conditions of 10,000 × *g*'s and ∼20,000 rpm and the fire test under the conditions of 43,000 × *g*'s and 57,000 rpm, the fabricated MRB has showed a maximum voltage of 34.6 ± 0.4 V, an activation time of 8.6 ± 0.6 ms and a maximum capacity of 37.4 ± 0.4 W s. Through experimental studies, the activation time of the MRB at a low temperature of −32 °C has been improved by decreasing the flow resistance of the electrolyte despite a decrease in ion mobility. The shock survivability of the fabricated MRB in gunfire environments also was experimentally verified.

Acknowledgements

The authors are grateful to Sung-Su Choi of the Hanwha Corporation, Gumi, Republic of Korea, for his technical support in

characterizing the prototype miniaturized *g*- and spin-activated $Pb/HBF_4/PbO_2$ reserve batteries.

References

[1] Nomenclature and Definitions in the Ammunition Area, MIL-STD-444, U.S. Department of Defense, 1963, pp. 75–82.

[2] L. Lorant, N. Johnson, Sidewinder turvine-driven generator, in: Proceedings of Symposium on Auxiliary power for Guided Missiles, 1957.

[3] K.H. Kim, Y.H. Lee, S.W. Lee, Energy Storage Characteristics and System Design of a Piezo-Generator for Small-Arm Fuze, Technology Report, TEDC-419-011191, Agency for Defense Development, 2001.

[4] S.-H. Yoon, J.-S. Oh, Y.-H. Lee, S.-W. Lee, Miniaturized inertia generators as power supplies for small-caliber fuzes, IEEE Trans. Magn. 41 (2005) 2300–2306.

[5] K.B. Lee, L. Lin, Electrolyte-based on-demand and disposable microbattery, J. Microelectromech. S 12 (2003) 840–847.

[6] R.M. LaFollette, J.N. Harb, L.G. Salmon, D.M. Ryan, The performance of microscopic batteries developed for MEMS applications, in: Proceedings of the 33rd Intersociety Engineering Conference, Colorado Springs, 1998.

[7] L.G. Salmon, R.A. Barksdale, B.P. Beachem, Development of rechargeable microbatteries for autonomous MEMS applications, in: Proceedings of Solid-State Sensor and Actuator Workshop, Hilton Head Island, 1998.

[8] Test Method Standard for Environmental Engineering Considerations and Laboratorial Tests, MIL-STD-810E, U.S. Department of Defense, 1989, pp. 501.3.1–502.3.14.

[9] M. Peabody, T. Griffin, K. Outt, Advanced lithium oxyhalide reserve battery for the M80 PIP proximity fuze, in: Proceedings of the 46th NDIA Fuze Conference, San Antonio, 2002.

[10] Design Criteria Standard: Safety Criteria for Fuze Design, MIL-STD-1316E, U.S. Department of Defense, 1998, pp. 8–13.

[11] W.S.N. Trimmer, Microrobots and micromechanical systems, Sens. Actuators 19 (1989) 267–287.

[12] J. Lee, C.-J. Kim, Surface-tension-driven microactuation based on continuous electrowetting, J. Microelectromech. S 9 (2000) 171–180.

[13] R.R.A. Syms, E.M. Yeatman, V.M. Bright, G.M. Whitesides, Surface tension-powered self-assembly of microstructures—the state-of-the-art, J. Microelectromech. S 12 (2003) 387–417.

[14] D. Berndt, Battery Technology Handbook, 1st ed., Marcel Dekker Inc., New York, 1989, pp. 1–27.

[15] D. Linden, T.B. Reddy, Handbook of Batteries, 3rd ed., McGraw-Hill, New York, 2001.

[16] S.-H. Yoon, Y.-H. Cho, High precision digital microflow controllers using fluidic digital-to-analog converters composed of binary-weighted flow resistors, J. Microelectromech. S 15 (2006) 967–975.

[17] N.A. Hampson, C.J. Bushrod, The discharge capacity of the lead-lead dioxide couple in fluoboric and hydrofluosilicic acid, J. Appl. Electrochem. 4 (1974) 1–6.

[18] S.-H. Yoon, J.-S. Oh, S.-S. Choi, A computational method for optimizing electrolyte volume in the series-stacked $Pb/HBF_4/PbO_2$ reserve battery, in: Proceedings of the 13th Seminar for the Advanced Ground Combat System, Daejeon, 2005.

[19] FLUENT 6.1 User's guide, Fluent Inc., New Hampshire, 2003, pp. 20.1–20.9.

[20] M.A. Duesterhaus, V.I. Bateman, D.A. Hoke, Shock testing of surface micromachined MEMS devices, in: Proceedings of the 47th NDIA Fuze Conference, New Orleans, 2003.